# A qualitative quantum rate model for hydrogen transfer in soybean lipoxygenase

S. Jevtic[1, a)] and J. Anders[2, b)]
[1)]*Department of Mathematics, Huxley Building, Imperial College, London SW7 2AZ, United Kingdom*
[2)]*College of Engineering, Mathematics and Physical Sciences, University of Exeter, Stocker Road, Exeter EX4 4QL, United Kingdom*

The hydrogen transfer reaction catalysed by soybean lipoxygenase (SLO) has been the focus of intense study following observations of a high kinetic isotope effect (KIE) in several experiments. Such findings demonstrate a departure from semiclassical rate theory. A contested issue is whether the transferring particle, hydrogen or one of its isotopes, hops over the reaction energy barrier or whether it *tunnels* through it. In this paper we build a qualitative quantum rate model that follows the non-equilibrium dynamics of the transferring particle when it is exposed to energetic potentials exerted by the donor and the acceptor. The enzyme's impact on the dynamics is modelled by an additional energetic term, an oscillatory contribution known as "gating". By varying two key parameters, the gating frequency and the mean donor-acceptor separation, the model is able to reproduce well the KIE data for SLO wild-type and SLO mutants over a large temperature range. The model allows the calculation of KIEs for future rate experiments with new SLO mutations, enabling a test of the predictive power of the model. While SLO-specific constants have been considered here, it is possible to adapt these for other enzymes.

arXiv:1612.03773v1 [physics.chem-ph] 9 Dec 2016

## I. INTRODUCTION

Enzymes play a central role in biological functions and are indispensable in many industrial processes[1]. As such, there is a pressing need to develop theoretical models that fully specify the method by which enzymes catalyse reactions. An enzyme creates an alternative path for a reaction to occur and can greatly speed up the reaction compared to the uncatalysed case; speed-up factors of up to $10^{26}$ have been observed[2]. As well as being able to simulate the data of known enzymes, it is crucial to find a model that can predict the action of a potential catalyst. This will enable the engineering of new enzymes for reactions that are currently too slow[3].

The standard method for modelling enzyme reaction rates is based on transition state theory (TST)[4]. In TST, the reactants begin in a local minimum of a potential $V(x)$, proceed along a "reaction coordinate" $x$, and at $x = x_b$ they encounter an energetic barrier of height $V(x_b)$. Thermal excitations from the environment enable the formation of a "transition state" at the top of the barrier, and crossing the barrier leads to the products being created, see Fig. 1. In this picture, the catalyst lowers the energy barrier increasing the likelihood for the transition state to be formed and the transferring particle to hop over the barrier. The "hopping" picture has recently been questioned due to a large body of experimental data suggesting that, in some enzymatic systems such as soybean lipoxygenase (SLO), hydrogen may tunnel through the barrier rather than hop over it. A comprehensive discussion of these enzymes is given in [5].

Tunnelling, a quantum phenomenon, typically occurs at low temperatures, and the transferring particle must be weakly coupled to the environment[6]. This is far from the biological regime where reactions occur in solution and at room temperature. While there is agreement that electron tunnelling is necessary for the function of proteins[7], the suggestion that hydrogen, with its mass around 2000 times bigger than the electron, may tunnel is the source of much controversy[5,8–10]. From a wave-particle duality perspective, the electron wavefunction is highly delocalised and can efficiently tunnel through biological barriers. In contrast, the hydrogen wavelength $\sim 0.6\,\text{Å}$ is narrower than a typical energy barrier with width $\sim 1\,\text{Å}$ [11], so tunnelling should be strongly suppressed.

In this manuscript, we present a rate model that aims to capture qualitatively the mechanism of hydrogen transfer in enzyme-catalysed reactions. The purpose of the model is to be able to predict the mass and temperature dependence of the transfer rate and derive expected (primary) kinetic isotope effects (KIEs) for various SLO mutants. To achieve this, we treat the dynamics of the transferring particle quantum mechanically. We further allow the enzyme to sample a range of donor-acceptor configurations through a classical vibrating motion, known as *gating*[12], which arises due to thermal excitations from the environment at temperature $T$. For concreteness, here we focus on hydrogen and deuterium transfer catalysed by the enzyme soybean lipoxygenase (SLO), and its mutants. We chose two independent quantities to parametrise the rate of transfer, the average donor-acceptor separation, $R_e$, and the gating frequency, $\Omega$. Our calculated KIEs show good agreement with the experimental KIE curves for WT SLO and four different SLO mutants reported in Refs [13, 14] over the measured temperature range of $5 - 50^{\circ}$C. The parameter choices provide insight into the physical features that affect the reaction rates and KIEs, such as the donor-acceptor configurations of SLO mutants in comparison to WT. We can also use the model to discuss the tunnelling contribution, and predict KIEs for new temperatures and new mutants.

The paper is organised as follows. In section II, we introduce the enzyme SLO, summarise the relevant experimental, and briefly discuss existing rate models. We present our new qualitative quantum rate model in section III and discuss the key results in section IV. In section V we comment on whether tunnelling plays a significant role in SLO enzyme catalysis.

[a)]Electronic mail: sania.jevtic@imperial.ac.uk
[b)]Electronic mail: janet@qipc.org

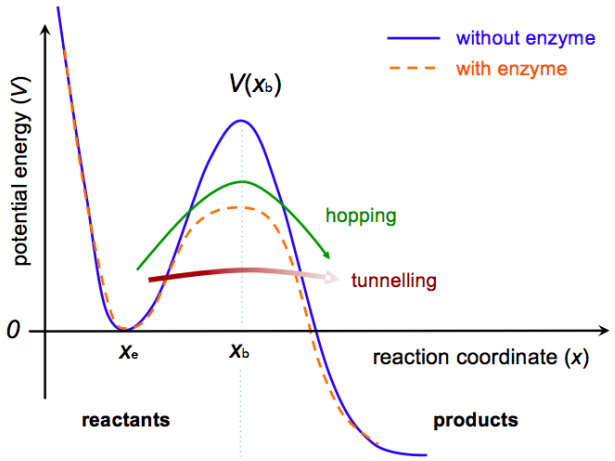


FIG. 1. Sketch of the potential energy profile $V(x)$ experienced by a particle transferring from a donor (reactants) to an acceptor (products). The particle, initially bonded to the donor, sits in a potential minimum at position $x_e$. The reaction proceeds along a reaction coordinate $x$ and at position $x_b$ a barrier of height $V(x_b)$ must be overcome if the particle is to break free of the donor and form a new bond with the acceptor. The particle may be thermally excited and hop over the barrier if the transfer is viewed classically, or it may tunnel through the barrier if it is governed by quantum dynamics. Enzymes are believed to catalyse the reaction by lowering the barrier height.

Section VI compares our rate model to the one used in [13]. Finally, in section VII, we provide a thorough discussion on what our model concludes about this chemical process and what we can predict, as well as suggestions for future directions.

## II. THE ENZYME SLO

Soybean lipoxygenase (SLO) is studied because of its similarities to the mammalian lipoxygenases. These are key components in the production of fatty acids which are required for the functioning of cells[15,16]. Abnormal lipoxygenase activity has been linked with cancer formation, hence these enzymes play an important role in human health and are of particular interest to the pharmaceutical industry[17–19]. SLO catalyses the production of fatty acid hydroperoxides and the substrate is linocleic acid[13]. The reaction consists of a sequence of rapid steps, however, the rate-limiting step is the hydrogen transfer from a carbon atom on linocleic acid to an oxygen molecule. This is the step that is modelled in our quantum dynamical rate model in section III.

### A. Kinetic isotope effect (KIE)

The first clear deviation from standard enzyme kinetics was reported in the kinetic isotope effect (KIE) of soybean lipoxygenase more than 20 years ago[20]. The KIE is an experimental tool for testing the mass-dependence of a reaction rate. It is the ratio between two rates: the rate of hydrogen transfer, $k_H$, and the rate of transfer of one of its isotopes, e.g. deuterium, $k_D$. (When the transferring particle is substituted by one of its isotopes this is called the primary KIE, and this is the situation we consider here. Secondary KIEs refer to rate changes that occur when isotopically substituting a non-transferring particle in the reactant.) The isotope substitution leads to negligible geometric and chemical differences: the extra neutron occupies very little space compared to the other reacting particles and it is chargeless. Hence, naively one might expect that the rate has no mass dependence and the KIE = $k_H/k_D = 1$. However, experimental SLO rates, shown in Fig. 2, exhibits a huge KIE = $k_H/k_D = 81$ at 30°C which has almost no temperature dependence over the accessible range of $5-50$°C. A number of rate models have been proposed that rationalise high KIE values, for a comprehensive review see [5]. A key conclusion is that high KIEs cannot be accounted for by semi-classical reasoning alone and require quantum corrections or even full quantum models.

### B. Mutations

Aside from deuterating the transferring particle, it is possible to *mutate* the enzyme by substituting large clusters of atoms ("residues") with smaller ones[13,14,21]. This is carefully done so that the enzyme catalyses the same reaction but the rate is altered. In [13], several "bulky" residues (leucine (Leu) 546 and 754, and isoleucine (Ile) 553) within the active site of SLO are replaced by the smaller amino acid alanine (Ala). Such mutations modify the active site and so hydrogen sees a different potential energy barrier. When the mutations change residues $\text{Leu}^{546} \to$ Ala (mutation M1) or $\text{Leu}^{754} \to$ Ala (mutation M2), which are both near the active site, both rates $k_H$ and $k_D$ significantly drop (about 3 orders or magnitude) in comparison to WT SLO, see Fig. 2. These findings indicate that wild-type SLO is configured optimally to catalyse this reaction. The KIEs of mutants M1 and M2 are larger than WT, 93 and 112 respectively at 30°C, and show stronger variation with temperature. In contrast, the more distant mutation $\text{Ile}^{553} \to$ Ala (mutation M3) barely changes the rates $k_H$ and $k_D$, see Fig. 2, but the M3 KIE is far more temperature dependent than the KIEs of WT and mutations M1 and M2. These observations were confirmed once more in [21]. Recently, kinetic data for the SLO *double mutant* (DM) have been obtained[14]. The double mutation makes both replacements M1 and M2 at the same time in SLO. Using two independent experimental methods, hugely inflated KIEs were observed: a KIE of $537 \pm 55$ at 35°C was measured using single-turnover kinetics and a KIE of $729 \pm 26$ at 30°C was measured using steady-state measurements.

### C. Other models of enzyme catalysis

It is known that enzymes with high KIEs, such as SLO WT and its mutants, with KIEs in the range 81 - 729, cannot be rationalised with classical transition state theories[5,22,23]. These theories model the transfer of hydrogen (or its isotopes) by

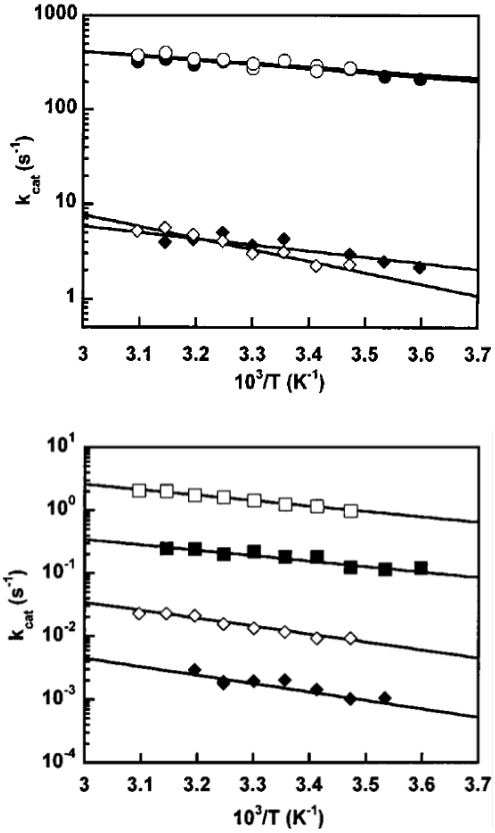


FIG. 2. Arrhenius plots of measured reaction rates over $10^3/T$ for SLO in the temperature $T$ range $5-50$°C. **Top:** Reaction rate data points for SLO wild-type (black symbols) and SLO mutation M3 ($Ile^{553} \rightarrow Ala$) (white symbols) for hydrogen transfer (circles) and deuterium transfer (diamonds). While the hydrogen transfer is not affected by mutation M3, the deuterium transfer is and this leads to a higher KIE for M3 than for WT. The solid lines are non-linear fits to the Arrhenius equation. **Bottom:** Rates for SLO mutation M1 ($Leu^{546} \rightarrow Ala$) (white symbols) and M2 ($Leu^{754} \rightarrow Ala$) (black symbols) for hydrogen (squares) and deuterium (diamonds) transfer. The data show that mutants M2 and M1 have significantly lower rates than WT, i.e. they are much less efficient in catalysing the reaction. Images taken from [13].

thermal excitation, i.e. hopping over the barrier, which can only produce small KIEs that are strongly temperature dependent. Higher KIEs require at least quantum corrections, such as the inclusion of the isotope dependent zero-point energy of the transferring particle in its initial potential[23]. Other quantum corrections include making the Wentzel-Kramers-Brillouin (WKB) approximation that treats tunnelling semiclassically, and/or using quantum perturbative methods, such as Fermi's golden rule[12]. However, for transfer distances of 1 $\AA$ and activation energies of $10^{-20}$J in SLO these approximations are not fully justified[24].

More recently, rate models have been developed that account for the increased complexity of the rate-determining step. These yield high KIEs, such as those observed in SLO, and reproduce their temperature dependence. For example, the rate model in [13] combines Marcus theory which is adapted to hydrogen transfer with *gating*[25,26]. Gating is the sampling of different configurations of the active site including close confinement where quantum tunnelling is possible[12]. This sampling is caused by the enzyme's thermal vibrating motion which reorganises the active site and modulates the barrier. The rate model in [13] reproduces the KIEs of WT SLO and two SLO mutants (M1 and M2). However, it does not account for the high temperature dependence of the KIE of mutant M3. Much effort has been devoted to experimentally determining whether enzymatic motion is really coupled to the active site configuration[27]. A number of rate models have adapted Marcus theory to accommodate hydrogen transfer and have been applied to SLO[25,26,28–30]. These theories originate from independent physical assumptions, but they all have two key features in common: hydrogen is treated quantum mechanically and the environment acts so as to organise the system into an arrangement that is conducive to tunnelling. These models provide a good fit to the wild-type SLO KIE data[13]. An intensive computational study was carried out in [31] using ensemble averaged variational TST with multidimensional tunnelling[32] to calculate the SLO rate and KIE. The authors reported that hydrogen tunnelling accounted for over 99% of the transfer mechanism in the wild type setting. The KIEs they obtain ($\sim 10$) are far lower than the observed value of 81. It is believed that this is due to an underestimation of the barrier height which comes from their computed hydrogen potential energy surface. Manually increasing the barrier height (and width) rapidly leads to an increased KIE.

These quantum-corrected models produce the observed KIE data. However, they are rather complex and require the fixing of many parameters. Rates calculated for different parameter choices are checked for consistency with the data, but the complexity of how the parameters affect the rates could limit the models' ability to make predictions for new experiments. Here we aim to develop a quantum rate model with limited complexity (two parameters) that qualitatively produces the observed KIEs and temperature variation. Varying the parameters allows us to predict the expected effect on KIEs for new experiments and glimpse insight in the physical mechanisms through which enzymes give rise to high KIEs and their observed temperature dependence. We present this qualitative rate model in the next section.

## III. A QUALITATIVE QUANTUM MODEL WITH CLASSICAL GATING

Building on previous rate models we propose here a new qualitative model for enzyme-catalysed hydrogen transfer that treats the dynamics of the transferring particle fully quantum mechanically. The model does not make semiclassical approximations, such as WKB or the Golden Rule. Instead the model calculates coherent quantum dynamics contributions to the rate. These contributions are then averaged over the active site configurations which are sampled by the enzyme's vibration (gating).

### A. Overview of the rate model

The model assumes that hydrogen, or one of its isotopes, is initially in thermal equilibrium in a potential $V^C$ created by the donor atom (carbon, C). When the acceptor atom (oxygen, O) is brought close by the enzyme, the hydrogen experiences a different potential, $V_R^{CO}$, which is parameterised by the donor-acceptor separation $R$. The hydrogen atom is out of equilibrium with the new potential $V_R^{CO}$ and this will result in quantum dynamics with the state of hydrogen evolving according to the Schrödinger equation. We obtain a quantum rate $\tau_R$ that quantifies the rate of the hydrogen transferring from the donor to the acceptor for each value of $R$. To obtain a prediction of the experimentally measured rate these quantum rates are then weighted with a classical gating probability $p(R)$ that determines the likelihood of the donor-acceptor distance $R$ being realised in a thermal environment[12]. The variation of this distance over a range $R_i \leq R \leq R_f$ is realised by the enzyme vibration, i.e. "gating". Averaging over the range of $R$ then gives the overall transfer rate,

$$k = \frac{N}{|R_f - R_i|} \int_{R_i}^{R_f} p(R)\, \tau_R \, \mathrm{d}R, \tag{1}$$

where $N$ is a dimensionless prefactor that characterises environmental effects in addition to gating and is in general temperature dependent. $N$ is independent of the mass of the transferring particle.

This rate expression allows one to predict the mass and temperature dependence of ratios of rates, i.e. KIEs, where environmental effects captured in the prefactor $N$ cancel out. The thermal vibrations of the enzyme influence the reaction by realising a configuration where the donor and acceptor are at a distance $R$ with probability $p(R)$. This probability will be a function of temperature and is determined by two parameters: the mean donor-acceptor distance $R_e$ and the gating frequency $\Omega$ of donor-acceptor oscillations about their equilibrium separation realised by the enzyme. The quantum rate $\tau_R$ derives from the Schrödinger equation of the transferring particle and is thus mass-dependent. In principle, $\tau_R$ is weakly temperature dependent, too, because of thermal occupation of the C-H bond energies before catalysis. However, as we will see this dependence is negligible at biological temperatures.

Aside from temperature and mass the parameters in this model are $R_e$ and $\Omega$. Choosing a specific hydrogen isotope, and thus the mass, fixes $\tau_R$. The only variables left to predict the KIEs for *all* SLO variants are then $R_e$ and $\Omega$, which determine the gating probability $p(R)$. The following subsections will discuss the factors $\tau_R$ and $p(R)$ and their parameter dependence in more detail.

### B. The quantum mechanical transfer rate $\tau_R$

Prior to the transfer event, hydrogen (H) or one of its isotopes, is bonded to the donor carbon (C) atom and in thermal equilibrium with its environment at temperature $T = (k_B\beta)^{-1}$. The initial state of hydrogen is thus the stationary, thermal state $\rho = \sum_{n=0}^{\infty} |E_n^C\rangle\langle E_n^C|\, e^{-\beta E_n^C}/Z_\beta^C$ of the C-H interaction potential $V^C$, where $E_n^C$ are the eigenenergies and $|E_n^C\rangle$ the energy eigenstates of $V^C$, and $Z_\beta^C$ is the partition function. However, in the biological temperature range $T \in [5°\mathrm{C}, 50°\mathrm{C}]$ the parameters that determine $V^C$, discussed in subsection III D, result in excited energy levels of $V^C$ that are too high to be significantly populated. Thus the hydrogen begins to a very good approximation (with over 99% probability) in the vibrational ground state $|E_0^C\rangle$ of the potential $V^C$. Therefore the rate $\tau_R$ will be determined solely by the ground state evolution and so is temperature-independent.

When the enzyme brings the donor and acceptor atoms into close confinement in its active site, the hydrogen becomes exposed to an asymmetric double well potential $V_R^{CO}$ due to its interaction with the nearby acceptor oxygen (O) atom. For the following discussion we will assume a fixed donor-acceptor distance $R$. The change of potential means that the energy eigenstates of the system change and the ground state $|E_0^C\rangle$ of $V^C$ turns into a superposition of energy eigenstates of the new potential $V_R^{CO}$. It is the occurrence of this superposition that causes quantum dynamics to ensue, instead of this remaining a static situation. Furthermore, since hydrogen is in a superposition of energy eigenstates, its energy is not sharp. The uncertainty in the energy of hydrogen implies that despite the donor and acceptor ground state energies being non-degenerate, as is assumed in Marcus theory, hydrogen still has a non-zero probability to transfer.

Assuming $V_R^{CO}$ is constant during the small transfer time window $t_{\max}$, then the state of the transferring hydrogen atom at intermediate times $t \in [0, t_{\max}]$ is

$$|\psi_R(t)\rangle = \exp\left(-i\mathscr{H}_R^{CO} t/\hbar\right) |E_0^C\rangle, \tag{2}$$

where $\mathscr{H}_R^{CO} = \frac{p^2}{2m} + V_R^{CO}$ is the Hamiltonian that generates the evolution from the initial ground state $|E_0^C\rangle$ and $m$ is the mass of the transferring particle. The potential $V_R^{CO}$ will be a double well potential for larger values of $R$, see Fig. 3, with further details for $V_R^{CO}$ described below. The probability of hydrogen transfer is the probability of observing it on the acceptor site at time $t$, $\varphi_R(t) = \int_{x_b}^{\infty} |\langle x|\psi_R(t)\rangle|^2 \,\mathrm{d}x$, i.e. the hydrogen is anywhere to the right of the barrier peak position $x_b$, see Fig. 1. If there is no barrier, which can occur when C and O are very close, then $V_R^{CO}$ has a single well and $x_b$ is defined as the position of the minimum of $V_R^{CO}$. Physically this means that, at large donor-acceptor distances, the transferring particle is strongly localised either at the donor or the acceptor, while at smaller distances it is shared between the two.

To obtain a rate constant we average the time-derivative of $\varphi(t)$ over the time window $t_{\max}$. This window is given by the timescale on which damping occurs in a typical environment. Here this is $\frac{\hbar}{\Delta E}$ where $\Delta E$ is the energy gap between the ground and first excited states of the C-H bond (or C-D bond for deuterium). The Schrödinger evolution of the hydrogen atom then gives rise to the rate

$$\tau_R = \frac{1}{t_{\max}} \int_0^{t_{\max}} \frac{\mathrm{d}\varphi_R(t)}{\mathrm{d}t}\, \mathrm{d}t = \frac{\varphi_R(t_{\max})}{t_{\max}}, \tag{3}$$

with $\varphi_R(0) = 0$.

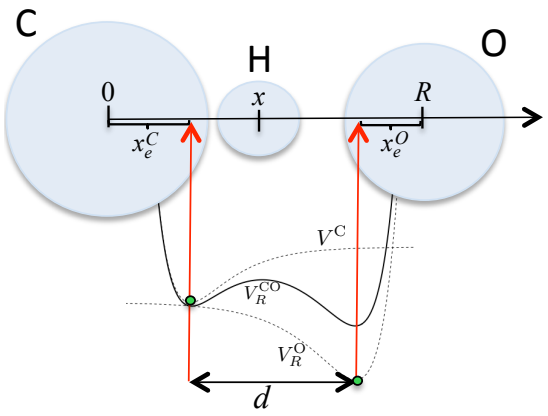


FIG. 3. The configuration of the donor carbon (C), transferring hydrogen (H) and acceptor oxygen (O) atoms. $x$ denotes the separation between H and C, while $R$ denotes the separation of O from C. The equilibrium internuclear separations of C-H ($x_e^C$) and O-H ($x_e^O$) are shown. They define the positions of the minima of the C-H and O-H Morse potentials, $V^C$ and $V_R^O$ (dashed black curves). The wells of $V^C$ and $V_R^O$ are separated by a distance $d$ and $V^C$ and $V_R^O$ are summed to give the asymmetric double well potential $V_R^{CO}$ (solid black line) experienced by H.

To calculate the rate $\tau_R$ we now detail the potential $V_R^{CO}$. It is composed of the two Morse potentials seen by the transferring particle due to the presence of the donor and acceptor. The Morse potential has the form $V^Y(x) = D^Y\left(1-e^{-g\,a^Y(x-x_e^Y)}\right)^2$ for each Y-H bond where Y is either C (donor) or O (acceptor). Here $D^Y$ is the well depth, $x_e^Y$ is the equilibrium separation and $a^Y = \omega^Y\sqrt{\mu^Y/2D^Y}$ is the well "curvature". $\mu^Y$ is the reduced mass between hydrogen and Y, and $\omega^Y$ is the bond frequency. These constants can be found in the literature for the case when only two particles, either C-H or O-H, are bonded. To account for the fact that the transferring particle before (after) the transfer sees the electrostatic potential not just of a single carbon (oxygen) atom, but of these atoms when part of donor (acceptor) molecule, the squeezing parameter $g$ has been introduced in $V^Y(x)$.

Assuming that the donor, hydrogen, and acceptor atoms are collinear in a single reaction coordinate $x$, see Fig. 3, the combined potential seen by hydrogen at C-O separation $R$ is $V_R^{CO}(x) = V^C(x) + V_R^O(x) - D^O$, obtained by summing $V^C(x) = D^C\left((1-e^{-a^C(x-x_e^C)}\right)^2$ and $V_R^O(x) = D^O\left(1-e^{-a^O(-x+(R-x_e^O))}\right)^2$ together with an offset $-D^O$. This offset guarantees that, if the acceptor (O) were moved infinitely far away from the donor (C), the hydrogen would feel no force due to the acceptor. The C-O separation is $R = d + x_e^O + x_e^C$, where $x_e^O$ and $x_e^C$ are fixed, and $d$ can vary, see Fig. 3. Note that $d$ defines the separation between the $V^C$ and $V_R^O$ well minima which can deviate from the well-separation of the two wells in the resulting $V_R^{CO}$.

While isotopes of hydrogen will have a different mass from hydrogen, this mass has no effect on the geometry of the system and on the electrostatic forces involved. Consequently, the potentials $V^C, V_R^O, V_R^{CO}$ remain the same for all isotopes. However, the eigenenergies and eigenstates of the corresponding Hamiltonians $\mathscr{H}^C, \mathscr{H}_R^O, \mathscr{H}_R^{CO}$ are mass-dependent, because mass enters the Schrödinger equation through the kinetic term $\frac{p^2}{2m}$. This is what makes the quantum contribution $\tau_R$, and therefore the overall rate $k$, dependent on the mass of the transferring particle. Denoting the hydrogen rate by $k_H$ and the deuterium rate by $k_D$, the KIE is the ratio $k_H/k_D$.

### C. Gating and the classical probability $p(R)$

Thermal energy from the environment causes the enzyme to vibrate. "Gating"[12] assumes that this enzyme motion is coupled to the active site configuration by making the donor (C) and acceptor (O) oscillate and sample a range of C-O separations $R_i \le R \le R_f$. The likelihood of a separation $R$ occurring is governed by the gating probability distribution $p(R)$. It is a Boltzmann distribution $p(R) = e^{-\beta U^{CO}(R)}/Z_\beta^{CO}$ for a potential $U^{CO}(R)$ that describes the sampling of donor-acceptor distances around a mean equilibrium position, $R_e$, at inverse temperature $\beta = 1/(k_B T)$, normalised by a partition function $Z_\beta^{CO}$. Assuming a quadratic potential, $U^{CO}(R) = \frac{\mu\Omega^2}{2}(R-R_e)^2$, results in a Gaussian gating probability $p(R)$. Here $\mu$ is the C-O reduced mass and $\Omega$ is the gating frequency. The standard deviation of distances sampled about the peak position $R_e$ is $\sigma = \sqrt{k_B T/(\mu\Omega^2)}$.

### D. Constants and parameters

In addition to varying temperature $T$ and isotope mass $m$, we will investigate how mutations of SLO from its wild-type affect the rates and the KIEs predicted with Eq. (1). Since mutants catalyse the same reaction, the functional form of the Morse potentials $V^C, V_R^O$ and $V_R^{CO}$ experienced by the transferring particle remain the same. However, the enzyme mutations will affect the equilibrium donor-acceptor distance, $R_e$, and the gating frequency, $\Omega$, of the gating distribution $p(R)$, and this determines the likelihood that a potential $V_R^{CO}$ will be seen by the transferring particle.

Constants for the C-H and O-H Morse potentials are available from standard chemistry data books[33]: the experimental dissociation energies 413 kJ/mol and 493 kJ/mol (measured from the zero point energies) are used to derive $D^C$ and $D^O$ (measured from the bottom of the well); the equilibrium distances are $x_e^C = 1.09$ Å and $x_e^O = 0.94$ Å; and the bond frequencies $\omega^C$ and $\omega^O$ are both 3000cm$^{-1}$ (in units of wavenumbers). The diatomic well curvatures $a^C$ and $a^O$ are calculated using these values. The squeezing parameter $g$ scales the width of the local electrostatic potentials seen by the transferring particle at the donor (and acceptor) in comparison to the widths of diatomic bonds. If the potentials $V^C$ and $V^O$ in the substrate are narrower in comparison to the isolated C-H and O-H bonds respectively, then the bond frequency in-

| SLO variant | $T$ (°C) | $R_e$ (Å) | $\Omega$ (cm$^{-1}$) | KIE Eq. (1) | KIE[13,14] | $N$ |
|---|---|---|---|---|---|---|
| WT | 30 | 2.9 | 402 | 81 | $81 \pm 5$ | $4 \times 10^{-6}$ |
| M1 | 30 | 2.95 | 375 | 93 | $93 \pm 9$ | $7 \times 10^{-8}$ |
| M2 | 30 | 2.95 | 387 | 112 | $112 \pm 11$ | $1.3 \times 10^{-8}$ |
| M3 | 30 | 3.05 | 324.8 | 93 | $93 \pm 4$ | $1 \times 10^{-4}$ |
| DM | 35 | 3.8 | 185.3 | 536 | $537 \pm 55$ | |
| DM | 30 | 3.8 | 185.3 | 696 | $729 \pm 26$ | |

TABLE I. Parameter values for reaction rates and KIEs for SLO WT and SLO mutants M1, M2 and M3 shown in Fig. 4 and for the double mutant DM. The KIE = $k_H/k_D$ predicted by Eq. (1) at temperature 30°C for each enzyme (and 35°C for the DM) is shown in column 5. The parameters $R_e$ and $\Omega$ have been chosen such that these KIEs match the experimental KIEs[13,14] which are listed in column 6. The prefactors $N$ have been chosen so that the rates match the data in Fig. 2. They set the scale for the rates but cancel out for KIEs. These choices and resulting KIEs are discussed in section IV.

creases and mathematically this is reflected in a value of $g > 1$. Here we choose $g = 2.3$ throughout.

The quantum transfer rate $\tau_R$ accounts for contributions from transitions between the ground state of the initial potential and various energetic states of the new double well potential. While theoretically all transfers will have a non-zero probability, environmental noise will limit the number of energetic levels that can be reached by the transferring particle. Here we choose to include transfers to the lowest 15 energetic eigenstates of the double well potential.

The donor-acceptor range $R_i \leq R \leq R_f$ governs which rate contributions are included in the rate Eq. (1). Recall that $R = d + x_e^O + x_e^C$ is determined by the distance $d$ between the $V^C$ and $V_R^O$ well minima. We assume that $d$ cannot be negative, i.e. C and O can be no closer than $R_i = x_e^C + x_e^O = 2.03$ Å. We choose the maximal value of $d$ to be 3 Å and so $R_f = 5.03$ Å. While this is the integration range we allow, in the end the probability $p(R)$ "controls" the window of C-O separations that are most relevant in the overall transfer rate $k$, see Eq. (1).

Physically it is reasonable for the isotope-independent rate prefactor $N$ to depend on the temperature as it reflects the environment's impact on the rate dynamics. To obtain a specific functional form will require a more detailed model of the environment, following for example Refs [34] and [29]. We here choose the rate prefactor $N$ to be constant for each SLO variant, see Table I. This choice sets a fixed scale for the rate plots **a)** and **b)** in Fig. 4. While these plots could be modified by a temperature dependent $N$, the relative behaviour of rates captured by KIEs, plotted in Fig. 4**c)**, are unaffected by $N$ even if it is temperature-dependent.

## IV. RESULTS

The hydrogen and deuterium transfer rates, $k_H$ and $k_D$, for all SLO WT and all SLO mutants are calculated with Eq. (1) using the values for the mean C-O separation $R_e$ and the gating frequency $\Omega$ listed in Table I. These parameter values are chosen such that the KIE at $T = 30$°C coincides with the experimental KIE data at that temperature, i.e. 81 for WT SLO, 93 for mutants M3 and M1, and 112 for mutant M2[13]. The parameter sets $R_e$ and $\Omega$ predict the average C-O separation and the width of the gating distribution $p(R)$. Multiple parameter sets can give the same KIE at a single temperature. For Table I we have chosen parameter sets that have physically reasonable values $2.7\ \text{Å} \leq R_e \leq 3.8\ \text{Å}$ and $\Omega \lesssim 400$ cm$^{-1}$, and which produce a KIE temperature dependence that resembles the experimental observations.

Fig. 4 displays the resulting Arrhenius rate plots for **a)** SLO wild-type (WT) and its mutant M3, and for **b)** SLO mutants M1 and M2. The temperature range shown is $5°\text{C} \leq T \leq 50°\text{C}$ in increments of 5°C. Fig. 4**c)** shows the corresponding KIEs for WT SLO and SLO mutants M1, M2, M3 as a function of inverse temperature. Comparing the predicted KIEs with the ratio of the experimentally measured rates, we find excellent agreement of the KIE gradient for SLO WT and its mutants M1 and M2. The agreement for the distant mutant M3 is less good: choosing values for $R_e$ and $\Omega$ close to those of WT makes the M3 and WT hydrogen rates very similar, in agreement with the experimental findings, however, the predicted M3 deuterium rate does not vary as strongly with temperature as the experimentally observed one. Nevertheless our parameters produce a M3 KIE that is the most temperature dependent of WT, M1 and M2, in agreement with experiment.

The parameters used to calculate the WT SLO rates shown in Fig. 4**a)** and WT KIE shown in Fig. 4**c)** are $R_e = 2.9$ Å and $\Omega = 402$ cm$^{-1}$. Any smaller value of $R_e$ would require a higher $\Omega$ and result in a very small gating width $\sigma$ of less than 0.08 Å. Gating frequencies are not expected to be greater than 400 cm$^{-1}$, which is the value used for the rate simulation in [13]. For M3 our equilibrium separation, $R_e = 3.05$ Å, is 0.15 Å higher than that of WT, 2.95 Å. This is a much smaller difference than the values used in the rate simulation in [13], where the equilibrium separation $R_e$ of M3 was 0.4 Å higher than the WT. This previous simulation for M3 was not able to produce as pronounced a KIE temperature dependence as observed experimentally. When we tried a large average separation of $R_e = 3.3$ Å in our model the temperature variation of both the H and D rates was much stronger and did not fit the experimental rates well. We believe a smaller difference better reflects the fact that mutant M3 is distant from the active site, and may not have such a significant effect on the equilibrium separation. To obtain the correct M3 KIE at 30°C the gating frequency had to be reduced from 400 cm$^{-1}$ for WT to 324.8 cm$^{-1}$ for M3. This leads to an increase in the standard deviation $\sigma$. Thus the gating distribution $p(R)$ at

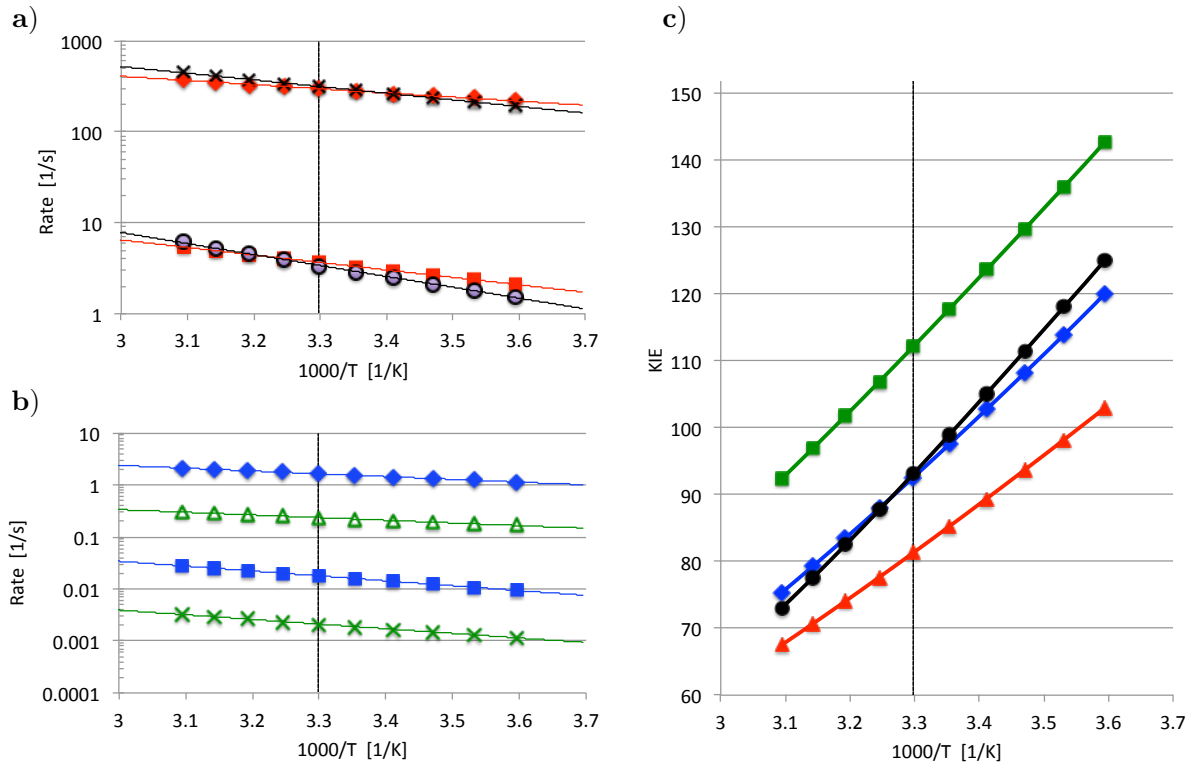


FIG. 4. Figures **a)** and **b)** show Arrhenius plots with trendlines of the transfer rates for SLO wild-type (WT) and its mutants M1, M2 and M3, with parameter choices given in Table I. **a)** The upper rates are for hydrogen transfer in WT (red, filled diamonds) and M3 (black, crosses). The lower rates are for deuterium transfer in WT (red, filled squares) and M3 (black, unfilled circles). **b)** From the top the rates are for hydrogen transfer in M1 (blue, filled diamonds), hydrogen transfer in M2 (green, unfilled triangles), deuterium transfer in M1 (blue, filled squares), deuterium transfer in M2 (green, crosses). Figure **c)** shows the corresponding KIE plots for SLO WT (red triangle), M1 (blue diamond), M2 (green square), and M3 (black circle) with trendlines. All plots are calculated with Eq. (1) using parameters given in Table I. The temperature is 30°C at $3.3 \times 1000/T$, indicated by the dashed lines.

30°C is determined by a peak and standard deviation given by $R_e \pm \sigma = 2.9 \pm 0.08$ Å for WT and $R_e \pm \sigma = 3.05 \pm 0.10$ Å for M3.

The rates calculated with Eq. (1) for SLO mutants M1 and M2 are displayed in Fig. 4**b)** and show excellent agreement with the experimental data in Fig. 2, bottom. Their KIEs are displayed in Fig. 4**c)**. To be obtain these curves we have chosen a mean C-O separation $R_e$ for M1 and M2 that is 0.05 Å greater than the mean separation realised by the WT SLO. This roughly matches the simulation parameters choices of [13]: M1 and M2 have the same $R_e$ which is slightly larger than the $R_e$ of WT. To match the experimental KIEs at 30°C we had to reduce the gating frequencies $\Omega$ of M1 and M2 by ca. 5% in comparison to WT, see Table I, and thus the sampling range increases slightly. Specifically, $p(R)$ for M1 is determined by $R_e \pm \sigma = 2.95 \pm 0.09$ Å and for M2 by $R_e \pm \sigma = 2.95 \pm 0.08$ Å. Note that it is the small decrease in gating range that leads to an increase of the KIE from 93 in M1 to 112 in M2. The KIEs of M1 and M2 are higher than WT and have a steeper temperature dependence (though are less steep than the M3 KIE), as expected from the experimental data in Fig. 2.

Finally, we compare KIE predictions of the developed model against the KIEs reported in a recent SLO double mutant (DM) experiment[14]. Here both the M1 and M2 mutations ($Leu^{546} \rightarrow Ala$ and $Leu^{754} \rightarrow Ala$) were implemented on a single SLO enzyme. Huge KIEs were observed with two independent methods for the same hydrogen transfer reaction: $537 \pm 55$ at 35°C using single-turnover kinetics and $729 \pm 26$ at 30°C using steady-state measurements. Large equilibrium separations are required to produce such inflated KIEs that vary by as much as 2 orders of magnitude over a 5°C temperature change. Using our model we choose the minimum donor-acceptor separation that is able to produce both KIE values at the respective temperature values. This minimum separation is $R_e = 3.8$ Å - much larger than if one added the effects of individual mutations on the distance, which each have an $R_e$ that is 0.05 Å greater than the WT. On the other hand, the corresponding gating frequency is $\Omega = 185.3$ cm$^{-1}$, see Table I. These parameter choices imply that the DM gating distribution, determined by $R_e \pm \sigma = 3.8$ Å $\pm 0.18$ Å, places the donor and acceptor much further apart than in single mutants and holds them in place less tightly than in WT. This suggests that the two mutations M1 and M2 together cause a rather signifi-

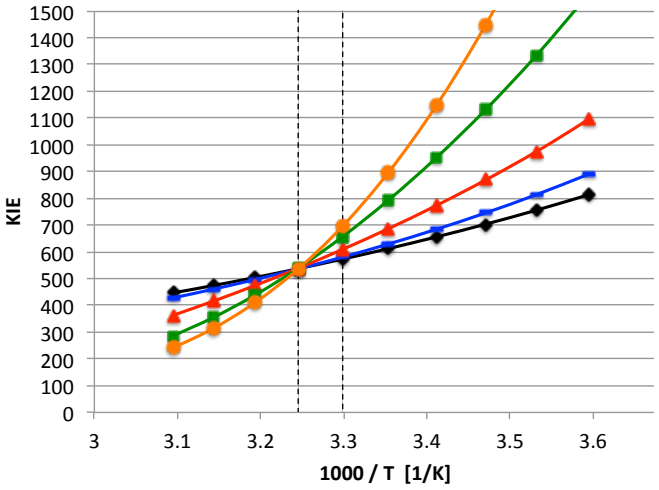


FIG. 5. KIE plots vs. inverse temperature calculated with Eq. (1) for various parameter choices, $R_e$ and $\Omega$, for SLO double mutant (DM)[14]. Black diamonds $(R_e,\Omega) = (3.4\text{Å}, 326.4\,\text{cm}^{-1})$, blue dash $(R_e,\Omega) = (3.5\text{Å}, 256.6\,\text{cm}^{-1})$, red triangles $(R_e,\Omega) = (3.6\text{Å}, 220.4\,\text{cm}^{-1})$, green squares $(R_e,\Omega) = (3.7\text{Å}, 199.8\,\text{cm}^{-1})$, and orange circles $(R_e,\Omega) = (3.8\text{Å}, 185.3\,\text{cm}^{-1})$. All choices are such that they reproduce the measured KIE of $537 \pm 2$ at 35°C. Dashed lines indicate the temperatures at which the rates have been measured, 30°C and 35°C.

cant modification to the active site.

The equilibrium separation value for the DM is 0.9 Å greater than the corresponding value for WT and it is not clear whether this captures the transfer situation in the DM well. Since the steady-state measurements method was found more reliable[14], we use the KIE value at 35°C as an anchor to identify other suitable parameter pairs. Fig. 5 shows the calculated KIE temperature dependence for alternative parameter pairs $(R_e,\Omega)$ that all give a KIE of $537\pm2$ at 35°C. These parameter sets have smaller separations, $R_e = 3.4 - 3.7$ Å but larger gating frequencies $\Omega$. The resulting KIE curves show that the temperature dependence is less pronounced than the measured KIE increase, which is reproduced only for the largest $R_e$ of 3.8 Å.

## V. TUNNELLING CONTRIBUTION

The presented model now allows us to decide if hydrogen tunnelling contributes to the observed rates. Hydrogen starts with a very high probability of over 99% in the energetic ground state $E_0^C$ of the donor potential $V^C$. It is then exposed to the combined donor-acceptor potential $V_R^{CO}$. At a given $R$, hydrogen tunnels if its initial energy $E_0^C$ is less than the height of the barrier of the potential $V_R^{CO}$. To quantify whether hydrogen tunnelling contributes significantly to the rate $k$ in (1) we identify the distance $\bar{R}$ that contributes most to it, i.e. $\bar{R}$ is the value of $R$ at which the product $p(R)\tau_R$ is maximised. For example, for WT SLO at 30°C the distance contributing most to the rate is found to be $\bar{R} = 2.68$ Å. At this distance the energy difference between barrier height and initial energy is $E_{\text{diff}} = V_{\bar{R}}^{CO}(x_b) - E_0^C \sim 0.52$ eV $\approx 12$ kcal/mol. We note that this energy barrier is an order of magnitude larger than activation energies obtained from an Arrhenius plot of the experimental data[13]. The chance that hydrogen is thermally excited from the ground state to the top of the barrier is exponentially supressed and hence it is highly unlikely that hydrogen hops over the barrier. Thus our model suggests that the dominant transfer mechanism is tunnelling.

## VI. COMPARISON TO ANOTHER RATE MODEL

Here we compare our proposed rate model with the one presented in [13] which is based on Marcus theory and adapted from [26] to fit the SLO data for the WT and mutants M1, M2 and M3[13]. The key isotope-dependent component of the resulting rates is a Franck-Condon term with a "dynamically-modulated tunnelling distance"

$$k \propto \int_0^{X_{\max}} F(X)P(X)\mathrm{d}X. \tag{4}$$

The integration variable $X = d\sqrt{m\Omega/\hbar}$ is proportional to the distance $d$ between the minima of $V^C$ and $V_R^O$, see Fig. 3. The integration range is $X \in [0, X_{\max}]$ where $X_{\max}$ is a free parameter. The function $F(X)$ is the static Franck-Condon term giving the overlap of donor and acceptor resonant vibrational levels as a function of the well separation $X$. $P(X)$ is the probability for the donor and acceptor be separated by $X$ and it is assumed a Gaussian peaked at $X_{\max}$. Integral (4) appears to be similar to our rate presented in Eq. (1), with the quantum rate $\tau_R$ playing the role of $F(X)$, and the classical gating probability $p(R)$ also Gaussian like $P(X)$. However, there are important distinctions. Firstly, there is no "resonance" condition on $\tau_R$ requiring that the donor and acceptor energy eigenstates must be degenerate in order for hydrogen to transfer. Secondly, the quantum rate $\tau_R$ and Franck-Condon term $F(X)$ are quite different. The calculation of $\tau_R$ assumes Morse potentials for the donor and acceptor whereas $F(X)$ make a harmonic approximation. Thirdly, a minor difference is that the integration in (4) is only performed over half of the Gaussian $P(X)$, whereas we integrate over a region around its maximum $R_e$ with the effect that larger separations also contribute to the KIE.

## VII. DISCUSSION AND FURTHER WORK

In this paper we investigated the hydrogen transfer reaction catalysed by soybean lipoxygenase. We developed a qualitative model that predicts the temperature dependence of the primary KIE through the rate $k$ given in equation (1). The model treats the dynamics of the transferring particle quantum mechanically resulting in $\tau_R$, a quantum contribution to the rate $k$. In addition it accounts for the enzyme's role in the transfer via a classical "gating" rate, $p(R)$, which arises because of the coupling of the enzyme's vibrations to the donor-acceptor separation.

The quantum rate $\tau_R$ is fixed by the type of chemical reaction, here the hydrogen (deuterium) transfer catalysed by SLO, and depends principally on the mass of the transferring isotope which will be crucial for the KIE. $\tau_R$ is determined by the double-well potential $V_R^{CO}$. One of the parameters that fixes its shape is the squeezing parameter $g$. If $V_R^{CO}$ were the sum of isolated diatomic C-H and O-H potentials, then $g$ would be 1. A larger $g$ makes the individual wells narrower and in our calculation we find that choosing $g = 2.3$ gives rate and KIE predictions that are in good agreement with experimental data for SLO WT and all mutants analysed here. This suggests that, when hydrogen (or deuterium) is bonded to the donor or acceptor in the presence of the substrate and the enzyme, then, during the rate-limiting step, hydrogen experiences a stronger attraction to either C and O. This slightly higher $g$ value of 2.3 produces a higher barrier in $V_R^{CO}$ and leads to enlarged KIEs. A similar finding was reported in the intensive computational study of SLO, where the barrier had to be manually increased to obtain KIEs that were as high as the experimental ones[31].

With the quantum part of the rate fixed, one is left with the classical gating rate $p(R)$ which is determined by just two free parameters. The donor-acceptor equilibrium separation $R_e$ and the gating frequency $\Omega$ set the average position and spread of the classical gating distribution $p(R)$. It is through changing these two parameters only that we obtain the various rates and KIEs of all the SLO mutants. We found that the model predictions show good agreement with the experimental data for physically reasonable choices of $R_e$ and $\Omega$, matching the values of the KIEs at 30°C as well as the temperature dependence of rates and KIEs. For example, to predict the KIE temperature dependence of the SLO double mutant we identified $R_e = 3.8$ Å and $\Omega = 185.3$ cm$^{-1}$ as a set of parameter values that match the experimentally observed KIEs at $T = 35$°C and $T = 30°$, and in particular produce the very high KIE increase of almost 200. We note that this parameter set predicts that the KIE of the DM at $T = 25$°C should be $\approx 900$. It would be very interesting to confirm or refute this KIE experimentally.

The general picture that emerges from this model is that in WT the active site is compressed and very rigidly held: its low $R_e$ keeps the donor and acceptor very close on average and its high $\Omega$ indicates little movement around the most likely separation $R_e$, with a spread $\sigma$ of less than 0.1 Å. As we saw in Fig. 4**c)** the WT parameter values, which are expected to be close to the "optimal" configuration for SLO, lead to KIEs in the range of 70-100 for biological temperatures with moderate temperature dependence. This suggests that $R_e$ and $\Omega$ are very finely tuned in the SLO WT.

In the mutants, a larger $R_e$ means that the carbon and oxygen are held further apart on average, and this opening of the active site effectively makes the barrier larger. Specifically, while the barrier height most likely seen by the transferring particle in WT is 35.2 kcal/mol at $R_e = 2.9$ Å, the most likely barrier height in M1 and M2 is 48.8 kcal/mol at $R_e = 2.95$ Å. The higher barrier in M1 and M2 makes the transfer even more difficult and very significantly lowers the rates of these mutants in comparison to WT. As well as an increase in $R_e$, a mutated SLO also has a decreased $\Omega$, implying that the donor and acceptor oscillate from their equilibrium separation over a larger range. The standard deviation $\sigma$ of the sampling distribution $p(R)$ depends on temperature and gating frequency as $\sigma \propto \sqrt{T}/\Omega$. The interplay of larger equilibrium separation and larger gating ranges results in large KIEs that have a much more pronounced temperature dependence than those of WT. The extreme case is the DM with a standard deviation of $\sigma = 0.18$ Å at 35°C.

We note that the quantum rate $\tau_R$ is large for small $R$, i.e. smaller separations result in much more efficient hydrogen transfer, and decays rapidly with $R$. This means that the separations which contribute significantly to the overall rate $k$ in Eq. (1) can be many $\sigma$ smaller than $R_e$. This was observed in section V, where we found that the separation $\bar{R}$ that contributes most to the rate $k$ can be much shorter than the most likely equilibrium separation $R_e$. This functional dependence makes the KIEs and their temperature dependence very sensitive to the values of $R_e$ and $\Omega$, particularly as these parameters take on higher values. Generally we find that the KIE increases when (i) $R_e$ is fixed while $\Omega$ is increased and (ii) when $\Omega$ is fixed but $R_e$ increases.

We conclude that while the model is quite simple in its structure and dependence on the particle mass and temperature, it qualitatively produces the rate/KIE behaviour observed in the KIE experiments we compared with for various SLO mutants. The model predictions for the temperature dependence of the KIE for the DM open the possibility to test the validity of the approach and model.

The values of physical constants in our model, such as the binding energies of hydrogen to donor and acceptor, are taken from experimental data, and chosen to match SLO. But it would be straightforward to replace them with relevant constants for other enzyme-catalysed reactions. Future research could thus address the modelling of rates and KIEs of other enzymatic systems that exhibit significant signatures of tunnelling, for instance the Old Yellow Enzyme family of flavoproteins[35] where particular attention is paid to the role of promoting vibrations. The KIEs of these enzymes are not as high as SLO but they are still larger than the semiclassical prediction. The observed KIEs also tend to be more temperature-dependent than SLO, and this could be accounted for by our model by, for instance, choosing a higher $R_e$ and lower $\Omega$ than the SLO WT. Applying the quantum model to these enzymes thus provides a fruitful avenue for testing the importance gating frequency and transfer distance in enzymatic systems whose KIEs suggest a large tunnelling contribution.

## ACKNOWLEDGMENTS

It is a pleasure to thank Judith Klinman and her group for their hospitality and many insightful discussions. We are also very grateful to Nigel Scrutton and Sam Hay for their instructive comments, and to Tobias Osborne and his group for their hospitality. SJ is funded by an Imperial College London Junior Research Fellowship. SJ also acknowledges ERC grants QFTCMPS, and SIQS by the cluster of excellence

EXC 201 Quantum Engineering and Space-Time Research. JA acknowledges support by the Royal Society and EPSRC (EP/M009165/1).

[1] L. Stryer, J. Berg, and J. Tymoczko, *Biochemistry*, 6th ed. (San Francisco, 2006).
[2] D. Edwards, D. C. Lohmann, and R. Wolfenden, J. Am. Chem. Soc. **134**, 525 (2012).
[3] K. Hult and P. Berglund, Current Opinion in Biotechnology **14**, 395 (2003).
[4] H. Eyring and A. E. Stearn, Chemical Review **24**, 253 (1939).
[5] R. K. Allemann and N. Scrutton, *Quantum Tunnelling in Enzyme-Catalysed Reactions* (The Royal Society of Chemistry, 2009).
[6] M. Razavy, *Quantum Theory of Tunnelling* (World Scientific Pub Co Inc, 2003).
[7] C. C. Moser, C. C. Page, and P. L. Dutton, Phi. Trans. R. Soc. B **361**, 1295 (2006).
[8] S. Borman, C & EN Washington , 35 (2004).
[9] M. Greener, The Scientist (2005).
[10] P. Ball, Nature (news feature) **431**, 396 (2004).
[11] Y. Cha, C. J. Murray, and J. P. Klinman., Science **243**, 1325 (1989).
[12] W. J. Bruno and W. Bialek, Biophys. J. **63**, 689 (1992).
[13] M. J. Knapp, K. Rickert, and J. P. Klinman, J. Am. Chem. Soc. **124**, 3865 (2002).
[14] S. Hu, S. C. Sharma, A. D. Scouras, A. V. Soudackov, C. A. M. Carr, S. Hammes-Schiffer, T. Alber, and J. P. Klinman, J. Am. Chem. Soc. **136**, 8157 (2014).
[15] S. T. Prigge, J. C. Boyington, B. J. Gaffney, and L. M. Amzel, Proteins **24** (1996).
[16] S. T. Prigge, J. C. Boyington, M. Faig, K. S. Doctor, B. J. Gaffney, and L. M. Amzel, Biochimie **79**, 629 (1997).
[17] M. K. Yu, P. J. Moos, P. Cassidy, M. Wade, and F. A. Fitzpatrick, J. Bio. Chem. **279** (2004).
[18] N. Rioux and A. Castonguay, Carcinogenesis **19** (1998).
[19] T. W. Moody, J. Leyton, A. Martinez, S. Hong, A. Malkinson, and J. L. Mulshine, Exp. Lung. Res. **24** (1998).
[20] M. H. Glickman, J. S. Wiseman, and J. P. Klinman, J. Am. Chem. Soc. **116**, 793 (1994).
[21] M. P. Meyer, D. R. Tomchick, and J. P. Klinman, PNAS **105**, 1146 (2008).
[22] W. W. Cleland, M. H. O'Leary, and D. B. Northrop, *Isotope Effects on Enzyme-Catalyzed Reactions* (University Park, Baltimore, 1977).
[23] R. P. Bell, *The Tunnel Effect in Chemistry* (Chapman & Hall, 1980).
[24] The WKB approximation provides a good estimate of the tunnelling probability through a barrier when $\hbar/S \ll 1$. In this case the tunnelling probability is $\propto \exp(-2S/\hbar)$. The action $S = \int_a^b \sqrt{2m[V(x)-E]}dx$ is for a one-dimensional potential $V(x)$ that has a barrier in the range $a \leq x \leq b$, and the incident particle has energy $E$ and mass $m$. For the purposes of an order estimation, let us assume the barrier is rectangular, i.e. $V(x) = V$ for $a \leq x \leq b$ and zero otherwise. Then $S = (b-a)\sqrt{2m[V-E]}$. Typical parameters for the transfer distance $b-a \sim 1$ Å and for the activation energy $V-E \sim 1$ kcal/mol $\sim 1 \times 10^{-20}$ J (from SLO data in [13]). Hence $\hbar/S \sim 0.1$ indicating that the WKB regime is not a very good approximation.
[25] D. Borgis and J. T. Hynes, J. Phys. Chem. **100**, 1118 (1996).
[26] A. Kuznetsov and J. Ulstrup, Can. J. Chem. **77**, 1085 (1999).
[27] S. Hay and N. Scrutton, Nat. Chem. **4**, 161 (2012).
[28] E. Hatcher, A. V. Soudackov, and S. Hammes-Schiffer, J. Am. Chem. Soc. **126**, 5763 (2004).
[29] E. Hatcher, A. V. Soudackov, and S. Hammes-Schiffer, J. Am. Chem. Soc. **129**, 187 (2007).
[30] M. M. H. Olsson, P. E. H. Siegbahn, and A. Warshel, J. Am. Chem. Soc. **126**, 2820 (2004).
[31] I. Tejero, M. Garcia-Viloca, A. González-Lafont, J. M. Llucha, and D. M. York, J. Phys. Chem. B **110**, 24708 (2006).
[32] J. Pu, J. Gao, and D. G. Truhlar, Chem. Rev **106**, 3140 (2006).
[33] Y.-R. Luo, *Comprehensive handbook of chemical bond energies* (CRC press, 2007).
[34] J. P. Bothma, J. B. Gilmore, and R. H. McKenzie, New J. Phys. **12**, 055002 (2010).
[35] S. Hay, C. R. Pudney, and N. S. Scrutton, FEBS Journal **276**, 3930 (2008).